INTERNATIONAL JOURNAL FOR NUMERICAL METHODS IN FLUIDS
Int. J. Numer. Meth. Fluids **29**: 125–142 (1999)

A FULLY COUPLED NAVIER–STOKES SOLVER FOR CALCULATION OF TURBULENT INCOMPRESSIBLE FREE SURFACE FLOW PAST A SHIP HULL

B. ALESSANDRINI* AND G. DELHOMMEAU

Division Hydrodynamique Navale, Laboratoire de Mécanique des Fluides, Ecole Centrale de Nantes, BP 92101, F-44321, Nantes Cedex 3, France

SUMMARY

This paper deals with the calculation of free surface flow of viscous incompressible fluid around the hull of a boat moving with rectilinear motion. An original method used to avoid a large part of the theoretical problems connected with free surface boundary conditions in three-dimensional Navier–Stokes–Reynolds equations is proposed here. The linearised system of convective equations for velocities, pressure and free surface elevation unknowns is discretised by finite differences and two methods to solve the fully coupled resulting matrix are presented here. The non-linear convergence of fully coupled algorithm is compared with the velocity–pressure weakly coupled algorithm SIMPLER. Turbulence is taken into account through Reynolds decomposition and k–ε or k–ω model to close the equations. These two models are implemented without wall function and numerical calculations are performed up to the viscous sub-layer. Numerical results and comparisons with experiments are presented on the Series 60 $CB = 0.60$ ship model for a Reynolds number $Rn = 4.5 \times 10^6$ and a Froude number $Fn = 0.316$.

1. INTRODUCTION

This work started with a basic consideration: double model incompressible flow solution (without free surface effects) and free surface flow solution are fundamentally different. Double model flow admits multiple solutions for the pressure, all of which are clearly defined with a constant, and free surface flow has a strictly single solution for the pressure field. The non-invertibility of the pressure matrix is due to the infinity of discrete solutions for the double model flow. The existence of these solutions is ensured by a second member compatibility criteria, i.e. the global conservation of mass, and depends on boundary conditions. Free surface flow is driven by the same equations (mean momentum transport equation and mass conservation) and unity of solution is ensured through free surface boundary conditions only (in fact kinematic and normal dynamic conditions). The evident conclusion is that at least one free surface equation must be coupled with the pressure equation. The easiest and the most common way to achieve this is to implement normal dynamic conditions, such as the Dirichlet boundary condition, in the pressure matrix. Mathematically, however, this operator does not need boundary conditions and the only way to take the normal dynamic condition into

* Correspondence to: Division Hydrodynamique Navale, Laboratoire de Mécanique des Fluides, Ecole Centrale de Nantes, BP 92101, F-44321, Nantes Cedex 3, France.

CCC 0271–2091/99/020125–19$17.50

Received November 1997
Revised January 1998

account is to locally substitute the discrete pressure equation with the normal dynamic condition, and give up the local conservation of mass in the cell near the free surface, which is theoretically unacceptable. Nevertheless, software based on this method gives good results except near the wall-free surface singularity [1–4]. The solution consists of relaxing the free surface condition, no-slip condition, or the no-slip condition near the hull, which is not very suitable for the quality of results.

This problem can be avoided using one of two methods. The first one is to solve the pressure block coupled with kinematic condition to express the flux on the free surface as a function of the pressure. Then the pressure block becomes invertible and the unity of the pressure solution is ensured. The second way consists of solving the fully coupled linear system constituted by the momentum transport equations, the mass conservation (pressure equation) and the free surface boundary conditions. Unfortunately the most efficient iterative algorithms (CGSTAB + ILU preconditioning, GMRES, MultiGrid) are unable to invert this fully coupled system due to the ill-conditioned matrix. The solution is to modify the system using the free surface boundary condition to express the flux through the free surface (as in the first method). The condition number decreases and the system becomes invertible by iterative algorithm (Figure 1). The description of this last method is the main purpose of this paper.

However, solving exact free surface conditions in the whole domain up to the viscous sublayer is not the only reason to implement a velocity–pressure-free surface elevation algorithm. Weakly coupled algorithms such as SIMPLE, SIMPLER or PISO can be interpreted as two blocks relaxation algorithms, sufficient to obtain an approximate divergence-free solution but unable to find an accurate velocity–pressure coupled solution. Consequently, convergence saturation on non-linear residual (Figure 2) must be seen as ill velocity–pressure coupling and not as difficulties in solving non-linearities, even in turbulent flows where non-linear effects are strong. Figure 2 presents the non-linear convergence history during a time step using the SIMPLER algorithm and fully coupled algorithm to solve the linear system. Figure 2 shows that the convergence saturation of the SIMPLER algorithm is not due to non-linear effects but to velocity–pressure coupling because of the fast convergence of fully coupled algorithm.

The conclusion is that the fully coupled method is a more accurate and faster way to solve Navier–Stokes equations with free surface conditions. We propose to solve the three-dimen-

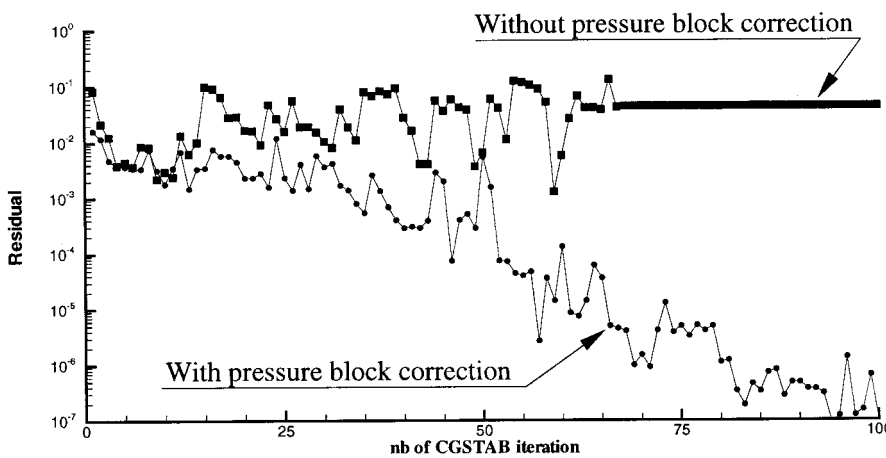

Figure 1. CGSTAB + ILU preconditioning convergence solving modified and non-modified fully coupled system.

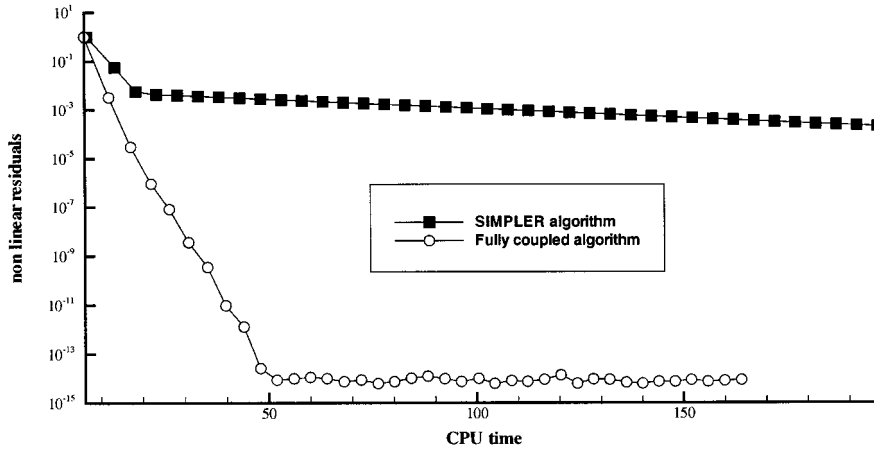

Figure 2. Comparison between fully coupled and SIMPLER algorithms to solve non-linear problem during a time step.

sional Navier–Stokes and Reynolds equations, with Newtonian closure, written in the convective form in a curvilinear computational space, fitted at each time to the hull and the free surface. k–ε and k–ω models solving two transport equations for kinetic energy and turbulence dissipation are compared. Near the hull a Jones–Launder low Reynolds formulation has been developed for the k–ε model. The main boundary conditions are the no-slip condition on the hull and the fully non-linear free surface conditions written on the actual position of the free surface. A dual unknowns location on the volumic grid associated to the Rhie–Chow interpolation technique is used for the construction of pressure equation. The three components of velocity are located on the nodes of the grid, pressure at the centre of elementary volumes and free surface elevation at the centre of free surface interface. Transport equations are written on the nodes of the mesh, the pressure equation is solved at the centre of elementary volumes and normal dynamic free surface condition at the centre of the free surface interface. The two tangential dynamic conditions and the kinematic condition form the set of velocity boundary conditions on the free surface. The fully linear system obtained by second-order finite difference schemes for the velocity components, the pressure and the free surface unknowns is solved at each iteration using a multigrid method with three levels of grid or a CGSTAB + ILU conditioning algorithm.

Numerical results concerning the free surface elevation and the velocity field around a Series 60 CB = 0.60 ($Rn = 4.5 \times 10^6$, $Fn = 0.316$) show good agreement with experimental results. The problem of singularity of kinematic condition on the hull is solved well and we can calculate the formation of an unsteady meniscus near the wall in the whole boundary layer.

2. EQUATIONS

Navier–Stokes–Reynolds equations are written under a convective form for a three-dimensional turbulent flow in a Newtonian incompressible fluid. The three components of velocity (u^i), pressure (p) including the gravitational effects ($\rho g x^3$) and turbulent kinetic energy ($2/3\rho k$) are the dependant unknowns. Independent unknowns are the three directions of curvilinear co-ordinates (ξ^i) and the time (t), (x^i) is the Cartesian basis and Ua the forward velocity. The

curvilinear system is chosen to simplify boundary conditions on the hull and on the free surface. $\xi^2 = 0$ and $\xi^3 = 0$ are the equations of the wetted part of the hull and of the free surface respectively, at each time.

A partial transformation of the Cartesian space moving with time in a curvilinear computation space is then applied. The metric of this transformation uses covariant basis (a_i) and contravariant basis (a^i), contravariant metric tensor (g^{ij}), control grid functions (f^i) and deformation velocities of the computational domain (u_g^i). Transport equations in the frame moving with the hull are written

$$u^\alpha_{,t} + (a_i^j(u^i - u_g^i) - v_{\text{eff}} f^j - a_k^i v_{t,i} a_k^j) u^\alpha_{,j} + \frac{1}{\rho} a_\alpha^k p_{,k} - v_{\text{eff}} g^{ij} u^\alpha_{,ij} - a_k^i v_{t,i} a_j^\alpha u^k_{,j} + \delta_{1\alpha} U a_{,t} = 0, \quad (1)$$

and the continuity equation

$$a_i^j u^i_{,j} = 0. \quad (2)$$

3. TURBULENCE MODELS

A classical k–ε model given for completely developed turbulent flow does not allow to describe parietal flow where the turbulent viscosity is negligible versus molecular viscosity. The Jones and Launder model [11] allows the integration of transport equations up to the wall. It gives the damping function, describing attenuation of turbulence as a function of turbulent Reynolds number $Rt = k^2/(v\tilde{\varepsilon})$. In the curvilinear space (ξ^i, t) the two transport equations for k and $\tilde{\varepsilon}$ are

$$k_{,t} + \left(a_i^j(u^i - u_g^i) - \left(v + \frac{v_t}{h_k}\right) f^j - a_k^i \frac{v_{t,i}}{h_k} a_k^j\right) k_{,j} - \left(v + \frac{v_t}{h_k}\right) g^{ij} k_{,ij} - P_r + \tilde{\varepsilon} - E_k = 0, \quad (3)$$

$$\tilde{\varepsilon}_{,t} + \left(a_i^j(u^i - u_g^i) - \left(v + \frac{v_t}{h_\varepsilon}\right) f^j - a_k^i \frac{v_{t,i}}{h_\varepsilon} a_k^j\right) \tilde{\varepsilon}_{,j} - \left(v + \frac{v_t}{h_\varepsilon}\right) g^{ij} \tilde{\varepsilon}_{,ij} - C_{\varepsilon 1} f_1 \frac{\tilde{\varepsilon}}{k} P_r + C_{\varepsilon 2} f_2 \frac{\tilde{\varepsilon}^2}{k} - E_\varepsilon = 0. \quad (4)$$

Turbulent viscosity is given by

$$v_t = C_\mu f_\mu \frac{k^2}{\tilde{\varepsilon}}. \quad (5)$$

f_1, f_2 and f_μ are given as functions of the turbulent Reynolds number:

$$f_1 = 1, \qquad f_2 = 1 - 0.3 \exp(-Rt^2), \qquad f_\mu = \exp(-2.5/(1 + Rt/50)). \quad (6)$$

The production term and the two other source terms are given by the following expression, where n is the normal vector at the hull and Vt is the tangential velocity:

$$P_r = v_t a_j^k u^i_{,k} (a_j^l u^i_{,l} + a_i^l u^j_{,l}), \qquad E_k = -2v((\sqrt{k})_{,n})^2, \qquad E_\varepsilon = 2v v_t (Vt_{,nn})^2. \quad (7)$$

Numerical values of constants are

$$C_\mu = 0.09, \qquad C_{\varepsilon 1} = 1.44, \qquad C_{\varepsilon 2} = 1.92, \qquad h_k = 1, \qquad h_\varepsilon = 1.3. \quad (8)$$

Another transport equation formulation has been proposed by Wilcox, introducing a specific dissipation rate, defined as

$$\omega = \frac{\varepsilon}{k\beta^*}. \quad (9)$$

The partial transformation of this transport equation is

$$k_{,t} + \left(a_i^j (u^i - u_g^i) - (v + \sigma^* v_t) f^j - a_k^i \frac{v_{t,i}}{h_k} a_k^j \right) k_{,j} - (v + \sigma^* v_t) g^{ij} k_{,ij} - P_r + \beta^* \omega k = 0, \tag{10}$$

$$\omega_{,t} + \left(a_i^j (u^i - u_g^i) - (v + \sigma v_t) f^j - a_k^i \frac{v_{t,i}}{h_\varepsilon} a_k^j \right) \omega_{,j} - (v + \sigma v_t) g^{ij} \omega_{,ij} - \frac{\gamma \omega}{k} P_r + \beta \omega^2 = 0, \tag{11}$$

with

$$\begin{cases} \beta^* = 0.09; \quad \sigma = 0.5; \quad \gamma = \dfrac{5}{9} \\ \gamma^* = 1.0; \quad \sigma^* = 0.5; \quad \beta = \dfrac{3}{40} \end{cases}. \tag{12}$$

4. STANDARD BOUNDARY CONDITIONS

The previous formulation has boundary conditions for the velocity field, the kinetic energy and the turbulence dissipation. No other equation is needed to give pressure or free surface elevation on the boundaries. Particularly, there is no algebraic interpolation in the vicinity of the wall. We note Γ_c the hull, Γ_e the external boundary, Γ_a the symmetry plane and Γ_s the free surface.

We use the following boundary conditions for k and $\tilde{\varepsilon}$:

$$k = k_{\min} \quad \text{and} \quad \tilde{\varepsilon} = \tilde{\varepsilon}_{\min} \text{ on } \Gamma_e \cup \Gamma_c \cup \Gamma_s, \qquad \frac{\partial k}{\partial x^2} = \frac{\partial \tilde{\varepsilon}}{\partial x^2} = 0 \text{ on } \Gamma_a, \tag{13}$$

and for k and ω:

$$\begin{aligned} &k = k_{\min} \quad \text{and} \quad \omega = \omega_{\max} \text{ on } \Gamma_s, \qquad k = k_{\min} \quad \text{and} \quad \omega = Ua/l \text{ on } \Gamma_e, \\ &k = k_{\min} \quad \text{and} \quad \omega \sim \frac{6v}{\beta d^2} \text{ on } \Gamma_c, \qquad \frac{\partial k}{\partial x^2} = \frac{\partial \tilde{\varepsilon}}{\partial x^2} = 0 \text{ on } \Gamma_a, \end{aligned} \tag{14}$$

where l is the boat length and d the distance to the hull.

Experiments have shown that the turbulent viscosity is greatly damped on the free surface [6]. This fact justifies the boundary conditions given by Equations (13) and (14). However, the decrease is very local and its influence on the results presented in this paper is weak.

Boundary conditions for the velocity field on other boundaries than Γ_s are given by

$$\begin{aligned} &u^i = 0 \text{ on } \Gamma_c, \qquad u^1 = Ua, \qquad u^2 = u^3 = 0 \text{ on } \Gamma_e, \qquad u^2 = 0, \\ &\frac{\partial u^1}{\partial x^2} = \frac{\partial u^3}{\partial x^2} = 0 \text{ on } \Gamma_a. \end{aligned} \tag{15}$$

5. FREE SURFACE CONDITIONS

Boundary conditions on Γ_s are: one kinematic condition, two dynamic tangential conditions and one normal dynamic condition. The kinematic condition, coming from the continuity

hypothesis, expresses that the fluid particles of free surface stay on it. To write this condition in a curvilinear frame, we must remark that h is only a function of two independent variables on the surface. Noting (b^i), the contravariant basis of the metric bidimensional transformation, we have

$$h_{,t} + (b_i^j(u^i - u_g^i)h_{,j})_{(i,j)\in\{1,2\}} - u^3 = 0 \text{ on } \Gamma_s. \tag{16}$$

Numerical difficulties at the intersection of the hull with the free surface come from this equation. Both the no-slip condition and free surface condition must be satisfied on the intersection. If the no-slip condition is placed directly into the free surface equation without care, one can deduce that $\partial h/\partial t = 0$. This conclusion is not verified by experiment and shows the singular numerical behaviour of kinematic condition on the intersection [8,12]. Mathematically, the only way for the free surface to move is to become tangential to the hull. In this case, the value of the Jacobian of the transformation is zero and kinematic condition cannot be used on the hull.

Dynamic conditions are given by the continuity of strains at the free surface. If we suppose that pressure is constant above the free surface, the normal dynamic condition is

$$p - \rho g h - 2\frac{\rho v_{\text{eff}}}{|a^3|^2} a_i^3 a_j^3 a_j^k u_{,k}^i - \frac{\gamma}{r} = 0 \text{ on } \Gamma_s, \tag{17}$$

where γ is the superficial tension coefficient and r is the free surface medium curvature radius. The tangential dynamic conditions are simply given by a linear combination of first velocities derivatives:

$$a_{\alpha i} g^{j3} u_{,j}^i = 0. \tag{18}$$

6. THE NUMERICS

The discrete components of velocity (U_i^α), kinetic energy (K_i) and turbulence dissipation (E_i), (Ω_i) are located along the curvilinear co-ordinate lines defining the volumic grid (Ω), which allows the boundary conditions on $(\partial\Omega)$ to be written. Pressure unknown (P_k) is located at the centre of elementary volumes (Ωv) to ensure mass conservation without special treatment at the boundaries. Free surface elevation (H_k) is located at the centre of the free surface interfaces $(\partial\Omega si)$, avoiding the singularity of the kinematic free surface condition. $\partial\Omega s$ is the point of Ω belonging to the free surface only and $\partial\Omega b$ is the equivalent of $\partial\Omega s$ in $\partial\Omega$. Figure 3 shows the location of the unknowns.

All numerical schemes used in the remaining part of this chapter are second-order schemes.

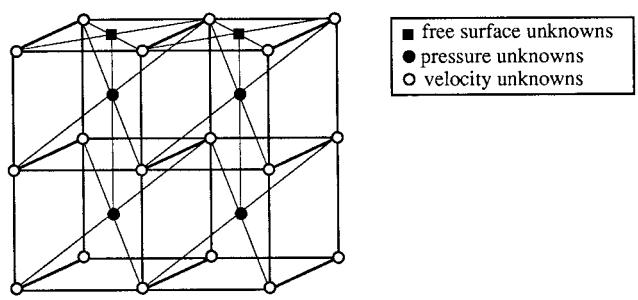

Figure 3. Location of unknowns.

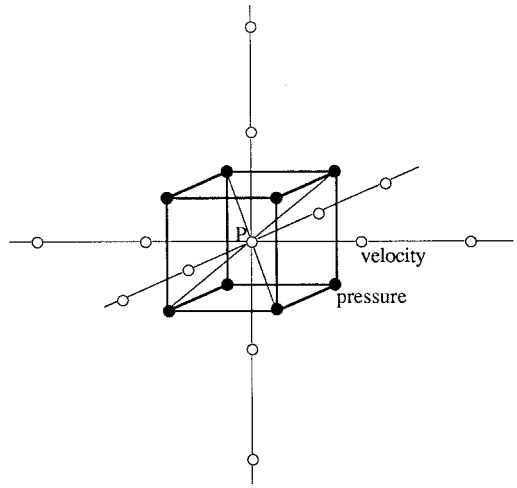

Figure 4. General discretisation cells.

6.1. Discretisation of transport equations

This discretisation needs a linearisation of equations: convection velocities and part of the turbulence terms are computed at the previous time step. Convection terms are computed with an upward second-order scheme and need a 13-point grid (Figure 4). Diffusion terms need a seven-point grid and the cross second derivatives (12-point grid) are in the source terms. Pressure gradient is computed on the nodes with an eight-point grid (Figure 4). So, at node i

$$U_i^\alpha + (\chi u)_{ij} U_{j\neq i}^\alpha + (\chi p)_{ik}^\alpha P_k = f u_i^\alpha \text{ on } \Omega \backslash \partial\Omega. \tag{19}$$

6.2. Discretisation of free surface conditions

Uncoupled methods use a classically kinematic equation to compute free surface elevation and dynamic normal condition, without viscous terms, such as a Dirichlet condition on the pressure. The problem of these methods has been described, so a very different algorithm is used here. The two tangential dynamic conditions associated with the kinematic condition give the three boundary conditions for velocities at the free surface and the normal dynamic condition allows the computation of the free surface elevation.

With this formulation, we linearise the kinematic condition as an implicit relation between the three velocity components and the free surface elevation:

$$h_{,t} + A^1 u^1 + A^2 u^2 - u^3 = A^1 u_g^1 + A^2 u_g^2. \tag{20}$$

Spatial derivatives of free surface elevation in the terms A^i are expressed with second-order centred schemes on a four-point grid. The unsteady term is computed by a three-point non-centred scheme. $\tilde{H}$ is the free surface elevation on the nodes of free surface given by interpolation of H (Figure 4), so the discrete expression of the kinematic condition is

$$\lambda_i^{1,1} U_i^1 + \lambda_i^{1,2} U_i^2 + \lambda_i^{1,3} U_i^3 + \eta_i^{1,4} \tilde{H}_i = f c c_i \text{ on } \partial\Omega s. \tag{21}$$

Discretisation of the two tangential dynamic conditions on a six-point grid can be written as

$$\begin{cases} \lambda_i^{2,1} U_i^1 + \lambda_i^{2,2} U_i^2 + \lambda_i^{2,3} U_i^3 + (\eta_{ij}^{2,1} U_j^1 + \eta_{ij}^{2,2} U_j^2 + \eta_{ij}^{2,3} U_j^3)_{j\neq i} = 0 \\ \lambda_i^{3,1} U_i^1 + \lambda_i^{3,2} U_i^2 + \lambda_i^{3,3} U_i^3 + (\eta_{ij}^{3,1} U_j^1 + \eta_{ij}^{3,2} U_j^2 + \eta_{ij}^{3,3} U_j^3)_{j\neq i} = 0 \end{cases} \text{ on } \partial\Omega s. \tag{22}$$

Equations (21) and (22) are free surface velocity field boundary conditions.

To obtain a well-conditioned system, we solve analytically, on each node, the linear system of Equations (21) and (22) for the unknowns U^i. The boundary conditions become

$$U_i^\alpha + (\chi su)_{ij}^\alpha U_{j\neq i}^\alpha + (\chi sh)_i^\alpha \tilde{H}_i = fs_i^\alpha \text{ on } \partial\Omega s. \tag{23}$$

It must be noted that a better conditioning of Equation (23) is obtained if the derivatives of the tangential dynamic conditions are not centred, to maximise the absolute value of coefficients λ^{ii}.

Discretisation of normal dynamic condition gives no problem. Viscous terms are explicit in the RHS. The only point to note is that the pressure is known at the centre of control volumes and the free surface at the centre of free surface interfaces. Pressure at the free surface is linearly extrapolated with a two-point scheme:

$$H_k + (\chi sp)_{kj} P_j = fh_k \text{ on } \partial\Omega si. \tag{24}$$

6.3. Discretisation of continuity equation, use of a generalised Rhie and Chow method to obtain the pressure equation

The Rhie and Chow method is commonly used to obtain a pressure equation without spurious modes, from the continuity equation. For the double model, this method gives an infinity of solutions differing by a constant, and the numerical solution needs the compatibility of the RHS. In the case of free surface problem, new boundary conditions ensure invertibility of the linear coupled system and unity of the solution. Unfortunately, due to the pressure block, numerical convergence is poor. A method giving an invertible and well-conditioned pressure block is used. All free surface conditions are explicitly introduced into the continuity equation for calculation of the divergence. Symbols with ($\sim$) or ($-$) above them are terms respectively interpolated on the nodes of the mesh or at the centre of free surface interfaces.

Free surface elevation is eliminated from Equation (23) using normal the dynamic condition (24):

$$U_i^\alpha + (\chi su)_{ij}^\alpha U_{j\neq i}^\alpha - (\chi sh)_i^\alpha (\tilde{\chi} sp)_{il} \tilde{P}_l = fs_i^\alpha - (\chi sh)_i^\alpha \tilde{fh}_i \text{ on } \partial\Omega s. \tag{25}$$

If we introduce the secondary unknowns ($U_i^{*\alpha}$), the three transport equations and three free surface conditions can be expressed at the centre of each interface (Ω_i) under the form

$$\bar{U}_n^\alpha - \bar{U}_n^{*\alpha} + \sigma_v (\bar{\chi} p)_{nk}^\alpha P_k - \sigma_s (\bar{\chi} sh)_n^\alpha (\chi sp)_{nj} P_j = 0 \text{ on } \Omega i, \tag{26}$$

with

$$U_i^{*\alpha} + \sigma_v ((\chi u)_{ij} U_{j\neq i}^\alpha - fu_i^\alpha) + \sigma ((\chi su)_{ij} U_{j\neq i}^\alpha - fs_i^\alpha + (\chi sh)_i^\alpha \tilde{fh}_i) = 0 \text{ on } \Omega, \tag{27}$$

and

$$\begin{cases} \sigma_v = 1 \text{ on } (\Omega \cup \Omega i) \backslash (\partial\Omega \cup \partial\Omega i) \\ \sigma_v = 0 \text{ on } \partial\Omega \cup \partial\Omega i \\ \sigma_s = 0 \text{ on } (\Omega \cup \Omega i) \backslash (\partial\Omega s \cup \partial\Omega si) \\ \sigma_s = 1 \text{ on } \partial\Omega s \cup \partial\Omega si \end{cases} \tag{28}$$

The pressure equation is obtained by writing the zero divergence on the control volumes. The case $\sigma_s = 0$ is the classical Rhie and Chow method, and gives an ill-conditioned system. Introduction of boundary conditions for the divergence calculation under free surface ($\sigma_s \neq 0$)

corrects the previous equation and gives a system which is easy to solve numerically. The pressure equation becomes

$$(\chi mp)_{kl} P_l + (\chi d)^{\alpha}_{ki} U_i^{*\alpha} = 0 \text{ on } \Omega v. \tag{28b}$$

7. SOLUTION OF LINEAR SYSTEMS

The coupled linear system matrix is

$$\begin{array}{|cccccccc|}
\hline
Id & & & -Id & & & \chi p & \\
 & Id & & & -Id & & \chi shp & \\
\chi cl & \chi cl & \chi cl & & & & & \\
\chi u & \chi u & \chi u & Id & & & & \\
\chi su & \chi su & \chi su & & Id & & & \\
 & & -Id & & & Id & & \\
 & & & \chi d & \chi d & \chi d & \chi mp & \\
 & & & & & & \chi sp & Id \\
\hline
\end{array}
\times
\begin{array}{|c|}
\hline
U/(\Omega \setminus \partial\Omega) \\
U/\partial\Omega s \\
U/\partial\Omega b \\
U^*/(\Omega \setminus \partial\Omega) \\
U^*/\partial\Omega s \\
U^*/\partial\Omega b \\
P/\Omega v \\
H/\partial\Omega si \\
\hline
\end{array}
=
\begin{array}{|c|}
\hline
 \\
 \\
fcl \\
fu \\
fssh \\
 \\
 \\
fh \\
\hline
\end{array}
\tag{29}$$

The linear system, which allows kinetic energy to be obtained and the turbulence to be dissipated, is solved independently.

Therefore, it is necessary to summarise the equations at each step to obtain velocities, pressure and free surface elevation. The transport equation is written on $\Omega \setminus \partial\Omega$ (19), the relation between the main and secondary unknowns on $\Omega \setminus \partial\Omega$ (23), the kinematic and tangential dynamic conditions on $\partial\Omega s$ (21), the implicit definition of secondary unknowns compatible with the values taken by σ_v and σ_s on $\partial\Omega$ (23), boundary conditions on velocities and the implicit relations for secondary velocity unknowns on $\partial\Omega$, the normal dynamic condition on $\partial\Omega si$ and the pressure equation on Ωv (24). It is important to note that no condition on pressure or free surface elevation is needed.

The main interest of the discretisation of the present method is that the velocity–pressure block is uncoupled with the free surface in the linear system. The solution for velocities and pressure can be obtained independently from free surface elevation, which can be computed at the end of each time step using the normal dynamic condition.

Linear system for turbulence kinetic energy and turbulence dissipation issued from turbulence models is first solved. This system is well-conditioned and easily invertible using a classical CGSTAB (accelerated and stabilised bi-conjugate gradient) without any preconditioning.

Unfortunately the fully coupled linear system for the velocities, pressure and free surface elevation unknowns is very ill-conditioned, especially the χmp block concerning the incompressible pressure equation, that means the mass conservation. So classical iterative methods are not available to solve this very large system. Two recent iterative methods have been tested in this paper.

The first method consists of an improvement in the CGSTAB algorithm using matrix preconditioning [16]. The second method is based on linear full multigrid algorithms [5]. Figure 5 presents the convergence of the two methods solving the fully coupled system. We can see

that the full multigrid algorithm is more efficient, but the difference between the CGSTAB algorithm and multigrid algorithms is less impressive than in two-dimensional model problems. Here the matrix structure and the grid complexity (very large aspect ratio near the hull, non-orthogonal lines) reduce the full multigrid efficiency.

8. NUMERICAL RESULTS

Numerical results of this method are presented here. Calculations are performed on a Series 60 $CB = 0.6$ hull for a Reynolds number $Rn = Ua \times l/v = 4.5 \times 10^6$, a Froude number $Fn = Ua/\sqrt{gl} = 0.316$ and a Bond number $Bn = \rho g l^2/\gamma = 1.3 \times 10^6$. The O–O topology grid (Figure 6) has 314265 nodes ($105 \times 73 \times 41$). The first grid point is located at $s/l = 1 \times 10^{-5}$ of the wall. To obtain a steady state, 300 time iterations are necessary with a non-dimensional time step $\tau = 0.02$. The CPU time is ≈ 20 h of a 20 specfp95 workstation.

Figure 7 shows the free surface elevation along the hull for two turbulence models (k–ε and k–ω) compared with experiments [14,15]. We can see that the influence of turbulence modelisation is weak, the two curves are superposed except on the wake, where the amplitude of the stern wave is larger with the k–ω modelisation. Experiments show an amplitude of the stern wave of ≈ 0.014, that seems in better agreement with the k–ω model.

Figure 8 shows that the wave field around the body is not strongly dependant on turbulence modelisation. Nevertheless, the damping of the oscillations in the wake seems to be smaller with the k–ω turbulence model.

It is well-known that for the conventional hull, coupling between viscous effect and wave field is weak except at the stern. For this reason, software based on the perfect fluid and zero vorticity flow assumptions solving Laplace equations by panel method gives good free surface elevation results [10], and the small influence of turbulence modelisation on the present

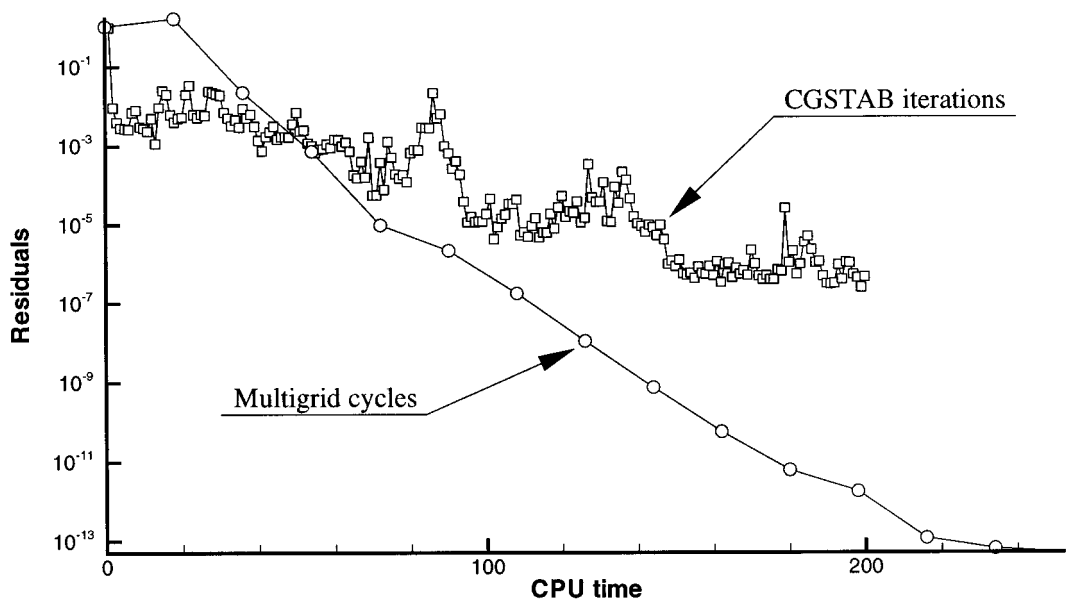

Figure 5. Comparison between CGSTAB and full multigrid algorithms.

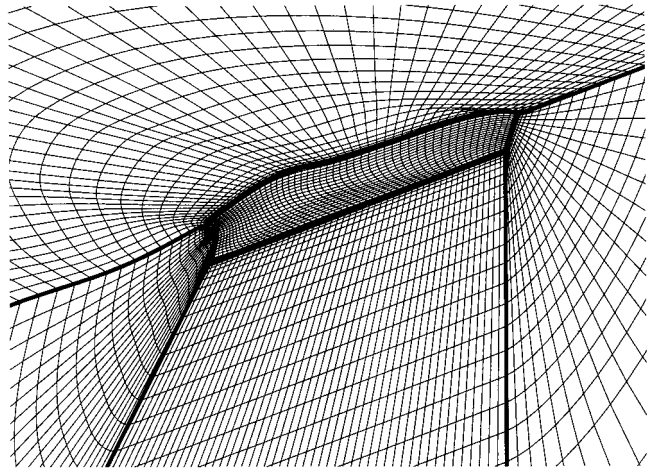

Figure 6. Grid topology around the hull.

calculation is not very surprising [7,9,13]. So to conjecture that vorticity is almost zero on the external region of the free surface seems reasonable. Nevertheless, numerical simulation shows that vorticity is significant in the boundary layer, which is a classical result, but also on the free surface, transported by gravitational effects, which is more astonishing (Plate 1).

Figures 9 and 10 present the longitudinal velocity isolines for experiments and the two turbulence models on various sections from the bow ($x/l = -0.5$) to the stern ($x/l = +0.5$). The $k-\varepsilon$ model gives a larger boundary layer thickness due to the convection of an open separation when the flow crosses the bilge ($x/l = 0.3$ and $X/l = 0.4$ sections). Isolines obtained with $k-\omega$ modelisation are in better agreement with experiments: the boundary layer thickness is well computed and does not increase excessively near the bilge. Figures 11 and 12 present the transversal and the vertical velocity components for $k-\omega$ modelisation. The agreement with the experiments is good for both components. We can note the location of the open separation on the $x/l = -0.1$, 0.1, 0.3, 0.4 sections.

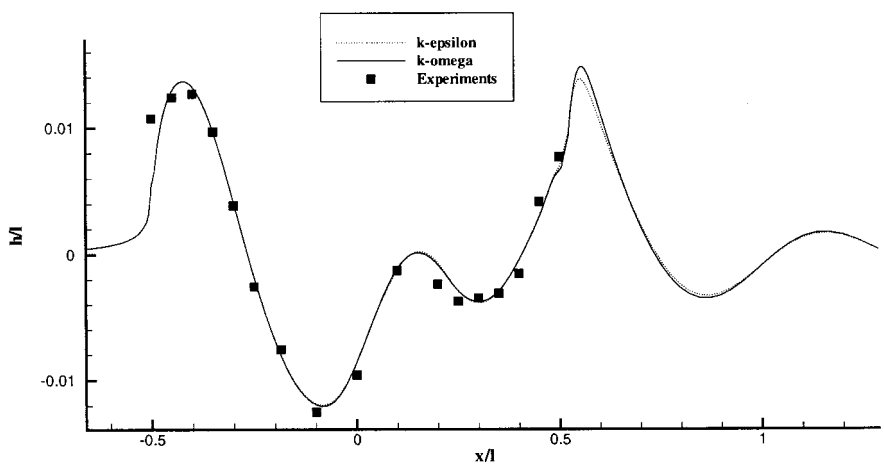

Figure 7. Free surface elevation along the hull for the two turbulence models.

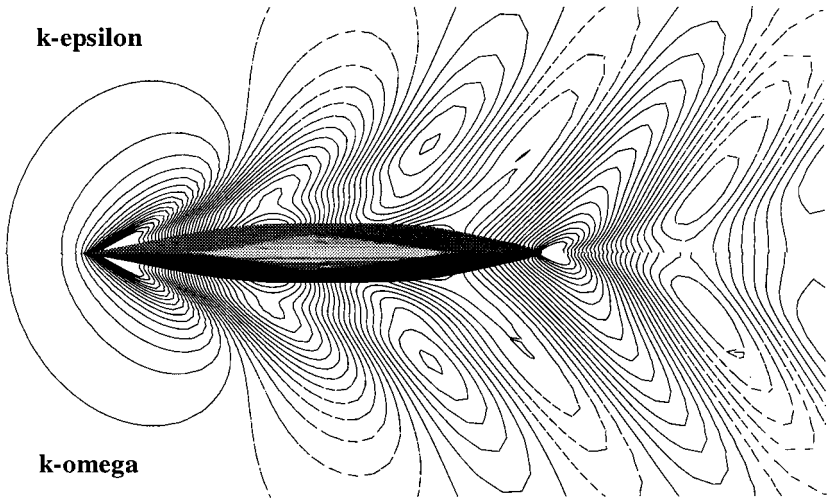

Figure 8. Wave field around the hull for the two turbulence models.

However, we have verified during calculations that boundary layer velocity profiles on the stern are strongly dependant on the transition between laminar and turbulent flow location. In the present calculations transition is imposed at $x/l = -0.47$.

An important topic for the future concerns the problem of bow wave breaking for fine discretisation. The first question is to determine the origin of this phenomenon: physical or numerical origin. Physically, two phenomena coexist: the problem of wave breaking concerning plunging breaker and spilling breaker and the problem of compatibility between no-slip boundary condition on the body and the kinematic condition on the free surface.

Astonishingly, spilling breaker does not appear to be a difficulty: two-dimensional calculation shows that numerical dissipation on the free surface increases with free surface slope and prevents the free surface from achieving breaking slope. In this case numerical dissipation acts like breaking dissipation. The problems of spilling breaker and jet on the bow is more problematic, the fast increase of vertical velocity on the free surface cannot be balanced by numerical dissipation and ends in the divergence.

The problem of compatibility between kinematic and no-slip condition appears to be very close to the hull for large Reynolds numbers ($Rn > 10^7$). The physical contradiction can be solved by forsaking the continuity hypothesis, that is out of place in this context. Mathematically, a numerical displacement of contact point is asymptotically ensured by tangency of the hull with the free surface. In any case, free surface elevation unknowns do not have to be located on the contact point.

Nevertheless, a free surface formulation allowing an accurate mass conservation and a strict discretisation of free surface conditions (and only free surface conditions, that is not always true) avoids a lot of numerical problems assimilated by error to wave breaking. Bow wave breaking does not appear for present flow parameters, but for higher Froude numbers or for computations of flows with attack angle, the wave breaking dissipation model should be absolutely necessary.

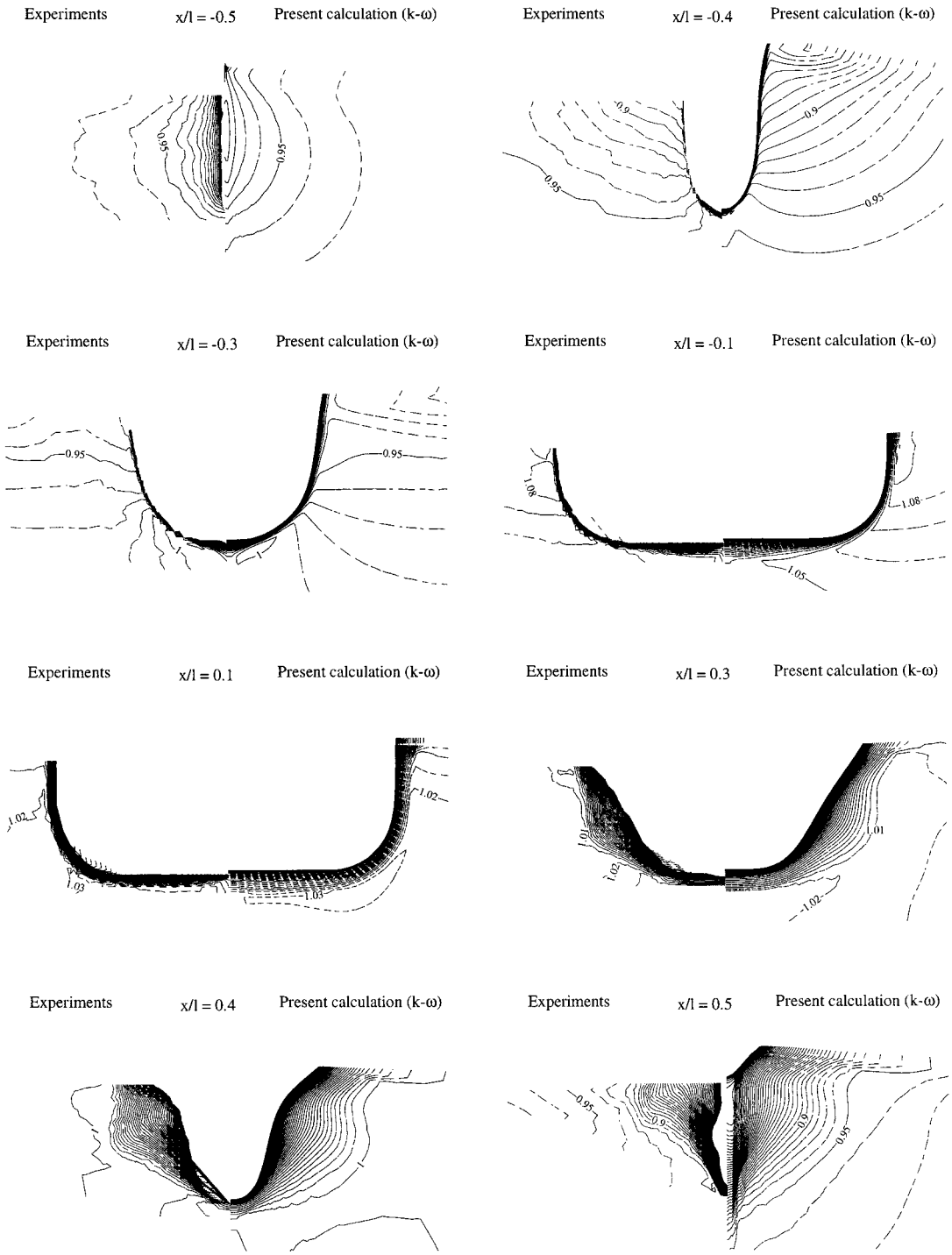

Figure 9. Longitudinal velocity component in various sections (k–ω model).

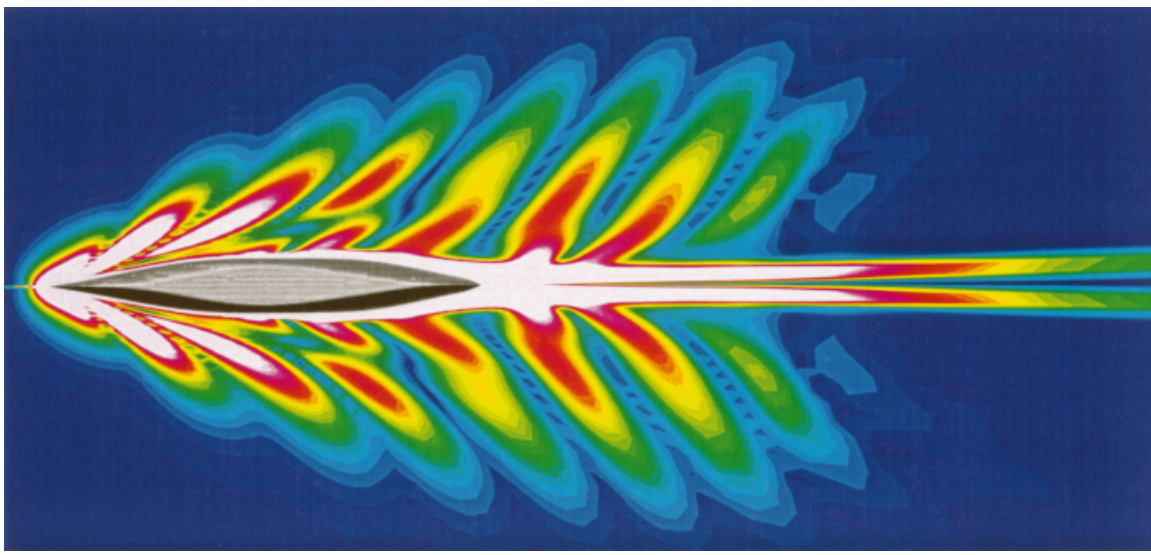

Plate 1. Flow vorticity on the free surface.

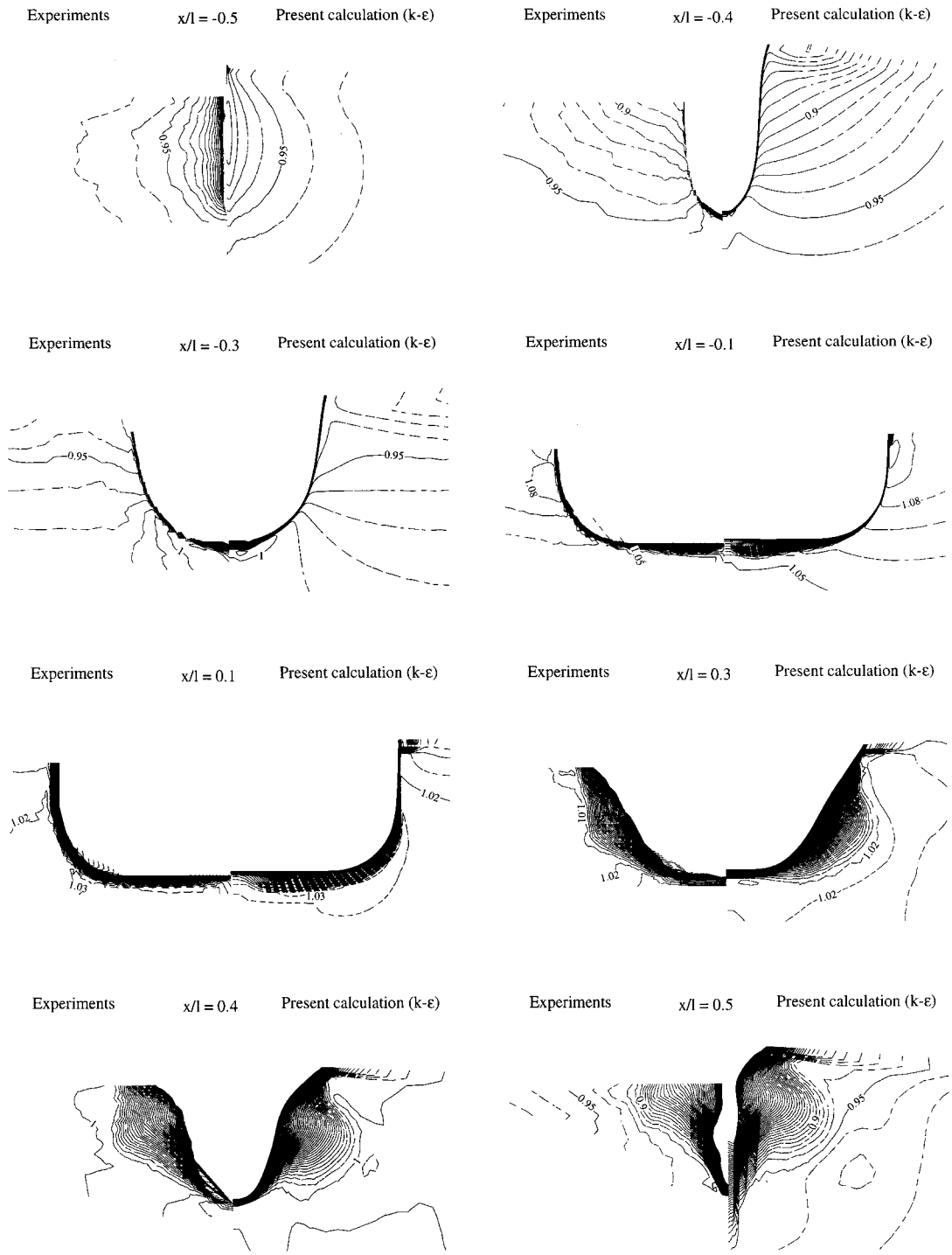

Figure 10. Longitudinal velocity component in various sections (k–ε model).

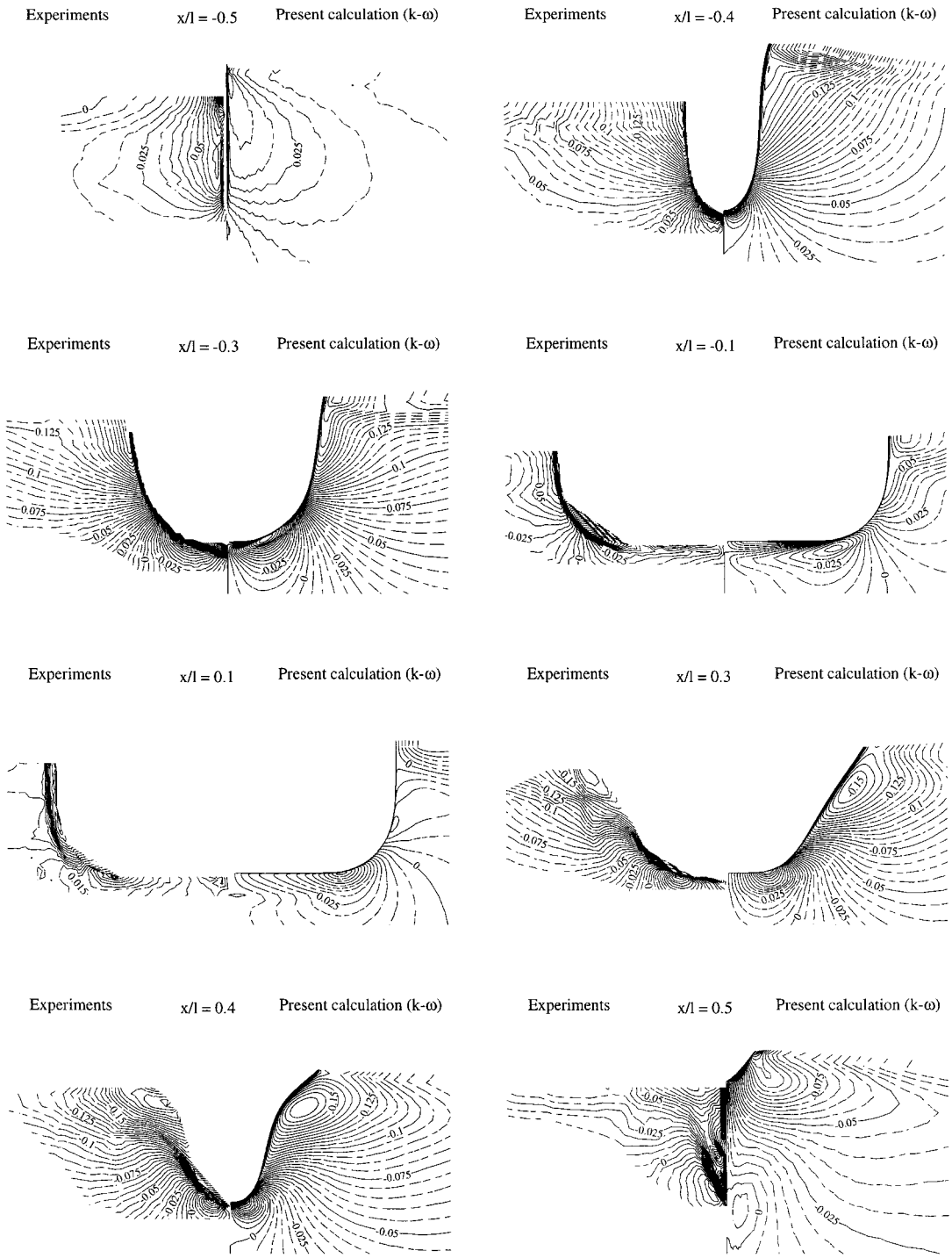

Figure 11. Transversal velocity component in various sections (k–ω model).

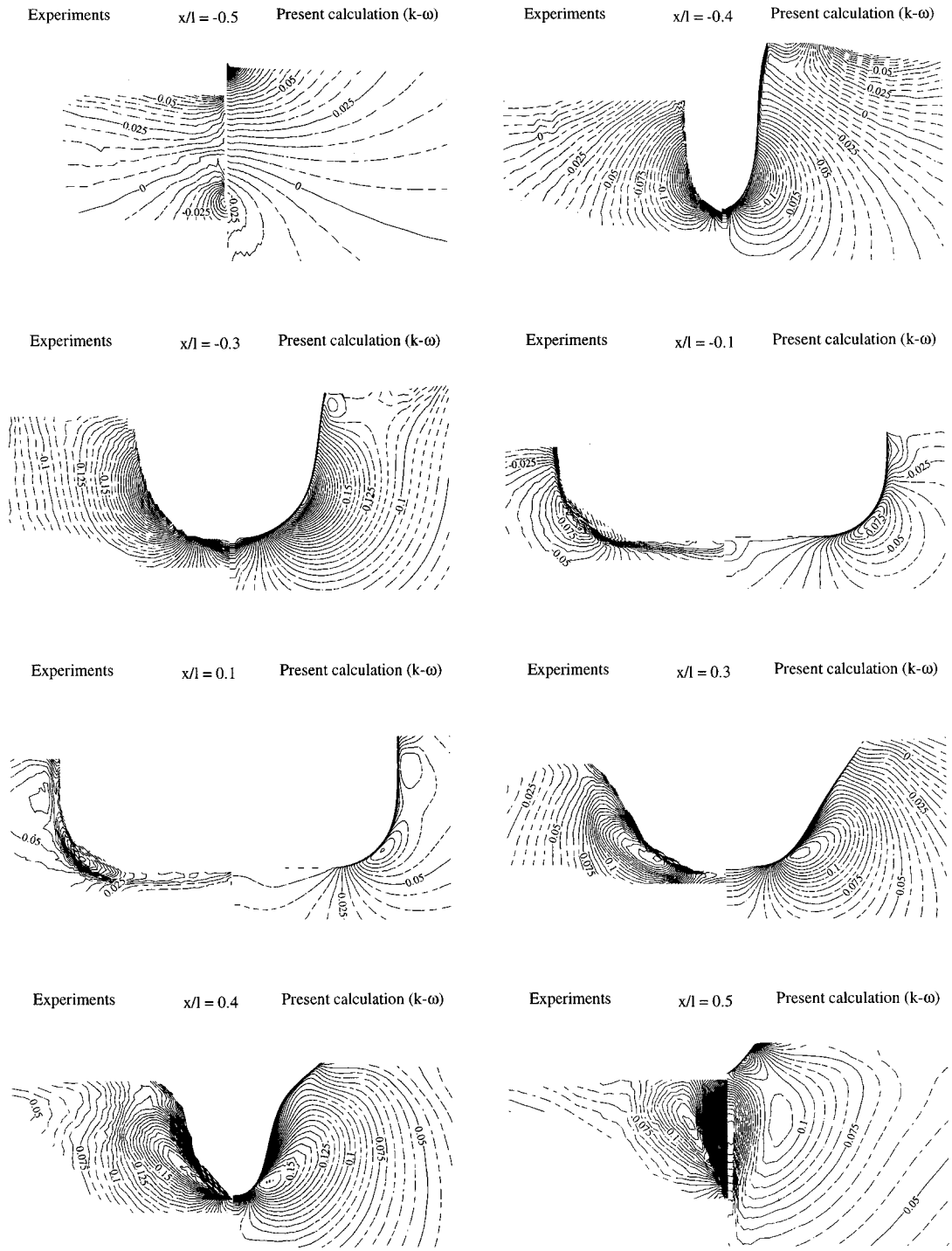

Figure 12. Vertical velocity component in various sections (k–ω model).

9. CONCLUSION

We have presented here a fully coupled algorithm allowing the solution of the Navier–Stokes–Reynolds equations with free surface effects. Physically, this method avoids the problem of mass conservation under free surface and significantly improves the treatment of wall-free surface intersection. Numerically this technique accelerates the velocity–pressure coupling: the fast convergence allows the solution of the linear system at the computer precision which was not possible using classical coupling algorithms (SIMPLE, SIMPLER, PISO) because of the very low convergence rate under a 10^{-3} residual.

The present method was tested on a well-known three-dimensional test case: the Series 60 $CB = 0.6$ for a Reynolds number equal to 4.5×10^6 and a Froude number equal to 0.316 with a k–ω turbulence model. The first computation grid node is located up to the viscous sublayer ($y+ < 5$) and all non-linear free surface conditions are solved on the whole domain. Concerning the wave field and the velocity fields, comparison of calculations and experimental results are in good agreement. The effects of a slight numerical damping on the wake are noted. Future work will be directed towards the resolution of this problem, perhaps using potential flow and RANSE coupling.

ACKNOWLEDGMENTS

The authors express their thanks to the French Direction des Recherches et Etudes Techniques (DRET) of the Délégation Générale pour l'Armement (DGA) which is supporting this work.

REFERENCES

1. B. Alessandrini and G. Delhommeau, 'Simulation of three-dimensional unsteady viscous free surface flow around a ship model', *Int. J. Numer. Methods Fluids*, **19** (1994).
2. B. Alessandrini and G. Delhommeau, 'Numerical calculation of three-dimensional viscous free surface flow around a Series 60 $CB = 0.6$ ship model', *CFD WORKSHOP*, Tokyo, March 1994.
3. B. Alessandrini and G. Delhommeau, 'A multigrid velocity–pressure-free surface elevation fully coupled solver for turbulent incompressible flow around a hull calculations', *9th Int. Conf. Numerical Method in Laminar and Turbulent Flow*, Atlanta, July 1995.
4. L. Gentaz, B. Alessandrini and G. Delhommeau, 'A fully coupled solver for two and three-dimensional incompressible and free surface flows in viscous fluid', *15th Int. Conf. Numerical Methods in Fluid Dynamics*, Monterey, June 1996.
5. B. Alessandrini and G. Delhommeau, 'A multigrid velocity–pressure-free surface elevation fully coupled solver for calculation of turbulent incompressible flow around a hull', *21st Symp. Naval Hydrodynamics*, Trondheim, June 1996.
6. I. Celik, W. Rodi and M.S. Hossain, 'Modelling of free surface proximity effects on turbulence', *Proc. Refined Modelling of Flows*, Paris, 1982.
7. H.C. Chen, W.L. Lin and K.M. Weems, 'Interactive zonal approach for ship flows including viscous and nonlinear wave effects', *6th Int. Conf. Numerical Ship Hydrodynamics*, Iowa City, August 1993.
8. E.B. Dussan V, 'On the spreading of liquids on solids surfaces: static and dynamic contact lines', *Annu. Rev. Fluid Mech.*, **11** (1979).
9. J. Farmer, L. Martinelli and A. Jameson 'Multigrid solutions of the Euler and Navier–Stokes equations for a series 60 $Cb = 0{,}6$ ship hull for Froude numbers 0, 160, 0, 220 and 0, 316', *CFD Workshop*, Tokyo, March 1994.
10. C.E. Janson, K.J. Kim and L. Larson 'Non-linear wave pattern calculation for the series 60 $CB = 0.6$ hull', *CFD Workshop*, Tokyo, March 1994.
11. W.P. Jones and B.E. Launder, 'The prediction of low Reynolds number phenomena with a two equations model of turbulence', *Int. J. Heat Mass Transf.*, **16** (1972).
12. E.E. Markovitch, 'Effect of free surface tension on the free outflow of a wetting fluid from a horizontal tube', Traduction of mekhanika Zhidkosti i Gaza, No 2, March–April 1988.
13. Y. Tahara and F. Stern, 'A large domain approach for calculating ship boundary layers and wakes for nonzero Froude number', *CFD Workshop*, Tokyo, March 1994.

14. Y. Toda, F. Stern and J. Longo, 'Mean-flow measurements in the boundary layer and wake and wave field of a Series 60 Cb = 0.6 ship model for Froude numbers 0, 16 and 0, 316', *IIHR Report No 352*, August 1991.
15. Y. Toda, F. Stern, I. Tanaka and V.C. Patel, 'Mean-flow measurements in the boundary layer and wake and wave field of a Series 60 Cb = 0, 6 ship model with and without propeller', *J. Ship Res.*, **34** (1990).
16. H.A. Vorst, 'Bi-CGSTAB: a fast and smoothly converging variant of Bi-CG for the solution of nonsymmetric linear systems', *J. Sci. Stat. Comput.*, **13** (1992).

